EMBEDDING DRUGS INTO MESOPOROUS SILICATES

Tina Ukmar[1], Gregor Mali[1], Odon Planinšek[2], Alenka Ristić[1], Miran Gaberšček[1], Venčeslav Kaučič[1]

[1]National Institute of Chemistry, Hajdrihova 19, 1000 Ljubljana, Slovenia

[2] Faculty of Pharmacy, University of Ljubljana, Aškerčeva 7, 1000 Ljubljana, Slovenia

E-mail: tina.ukmar@ki.si

INTRODUCTION

Among numerous applications of mesoporous silicates - ranging from separation technology to catalysis - they have recently been also recognized as very useful drug delivery devices [1-3]. Due to their biocompatibility and non-toxicity they can serve as carriers for drugs, enabling a diffusion controlled release under certain specific conditions. The porous network can serve as a reservoir for accommodation of drug molecules whereas the presence of surface silanol groups enables chemical functionalization to achieve the desired function. While most research focuses on the design of drug delivery systems which are sensitive to external stimuli and the resulting release kinetics of embedded drugs [4,5], the general relationship between silicate material properties, incorporation procedure and resulting drug loading is still not well established. Usually the loading into materials with varying pore sizes and pore volumes is performed with a universal technique whereby the center of attention is the total amount of embedded drug while the other differences in the resulting composite materials properties are of little interest. Therefore in our research we focused mainly on the relationship between the initial material properties, the loading solvent and the resulting material properties with respect to the amount of residual solvent, the total fraction of incorporated drug and the amount of drug potentially located outside the porous network. Indomethacin (an anti-inflammatory drug) was chosen as a model drug and was incorporated into SBA15 silicates with average pore sizes app. 6.7 nm and 9.9 nm.

EXPERIMENTAL

Synthesis of SBA15 matrix

Ordered mesoporous silicate with the average pore size of 6.7 nm (SBA15 (6.7)) was prepared with a classical hydrothermal synthesis using structure directing agent Pluronic P123 (triblock copolymer, Aldrich) and tetraethyl orthosilicate (98 % TEOS, Aldrich) as a silica source with the n_{TEOS}/n_{P123} ratio around 60. First Pluronic P123 was dissolved in the mixture of distilled water and hydrochloric acid (37 % HCl, Aldrich). This mixture was placed in an oil bath at 313 K under magnetic stirring. Then TEOS was added to the Pluronic P123 solution and stirred at the same temperature. The stirring was continued at higher temperature over night. Then the silica suspension was transferred into a Teflon-lined autoclave and placed in an oven for hydrothermal treatment at 373 K for 24 h. The obtained white powder was washed with distilled water, dried at 298 K and calcined at 823 K for 6 h in an air flow.
SBA15 with an average pore size of 9.9 nm (SBA15 (9.9)) was obtained with a modified synthesis procedure. The synthesis was the same as described above, except that before the stirring at higher temperature, a solution of poly(ethylene glycol) (PEG with Mn 1000, Sigma-Aldrich) as co-surfactant in 1.4 M HCl was added. The molar ratio $n_{P123}/n_{PEG1000}$ was 1.

Drug loading procedures of SBA15

First a saturated solution of indomethacin (IMC, Sigma) was prepared. Acetone and ethanol were used as loading solvents. After IMC was dispersed in the solvent, the resulting suspension was stored for 1 day to reach saturation. Then the saturated solution was filtered to remove the undissolved drug. The saturated solution was added dropwise to a layer of

SBA15. Equal amounts of solution were added to both SBA15 samples of equal masses. Prepared samples were then dried at 313 K for 24 h.

Materials characterization

X-ray powder diffraction (XRPD) patterns were recorded on a PANalytical X'Pert PRO high-resolution diffractometer with Alpha 1 configuration using CuK $_{\alpha 1}$ radiation (1.5406 Å) in the range from 0.5 to 5 ° 2θ and in the range from 5 to 40 ° 2θ. Micrographs were obtained by a Zeiss Supra^{TM} 35VP Scanning Electron Microscope (SEM) operated at 1 keV. Porosity was assessed with nitrogen sorption measurements using Micromeritics ASAP 2020 volumetric adsorption analyzer at 77 K. Before the adsorption analysis, the samples were outgassed under vacuum for 2 h at 473 K. The BET specific surface area (S_{BET}) was calculated from adsorption data in the relative pressure range from 0.04 to 0.20 for SBA15 (9.9) and from 0.04 to 0.16 for SBA15 (6.7). The total pore volume (V_t) was estimated from the amount adsorbed at a relative pressure of 0.989, converting it to the volume of liquid nitrogen at 77 K. The primary mesopore volume (V_{me}), microporosity (V_{mi}), external and total surface area (S_{ex} and S_t) were determined by α_s-plot method. The pore size distributions (PSD) were calculated from nitrogen adsorption data using BJH method. Differential Thermal Analysis with Thermogravimetric analysis (DTA/TG) was performed with STA 409C/CD (NETZSCH). Before DTA/TG the samples were dried under vacuum for 24 h at 313 K.

RESULTS AND DISCUSSION

First the structure and morphology of calcined SBA15 silicates were investigated. The XRPD patterns and PSD with adsorption isotherms of prepared SBA15 with different pore sizes are shown in Figure 1. XRPD patterns of both SBA15 samples show three maxima, which are assigned to the (100), (110) and (200) reflections of a hexagonal planar symmetry (Fig. 1 a).

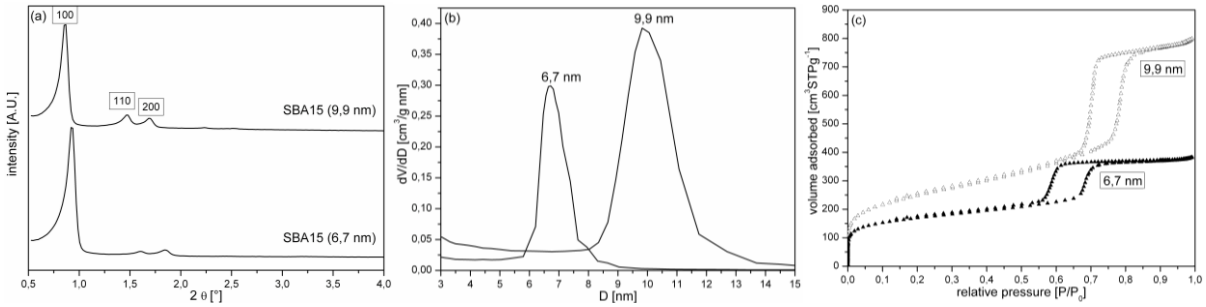

Figure 1: XRPD of calcined SBA15 silicates with different pore sizes (a) and pore size distributions (b) with corresponding adsorption isotherms (c).

Table 1: Structural properties of SBA15 (6.7) and SBA15 (9.9) samples

Sample	S_{BET} (m^2/g)	V_t (cm^3/g)	V_{me} (cm^3/g)	V_{mi} (cm^3/g)	S_{ex} (m^2/g)	S_t (m^2/g)	w_{BJH} (nm)
SBA15 (6.7)	606	0.59	0.45	0.07	40	388	6.7
SBA15 (9.9)	837	1.21	1.02	0.06	91	658	9.9

Structural characteristics obtained by sorption measurements are summarized in Table 1. The samples exhibit type-IV sorption isotherms typical for SBA15 silicates, that is, with narrow hysteresis loops of H1 type (Fig. 1 c). The nitrogen adsorption-desorption isotherms show steep increases of adsorption branches at p/p_o 0.78 - 0.84 for the sample SBA15 (9.9) and at p/p_o 0.68 - 0.76 for the sample SBA15 (6.7) due to the capillary condensation of nitrogen in the mesopores. These results indicate that the sample SBA15 (9.9) possesses larger mesopores than the sample SBA15 (6.7). This finding is proved by a larger BJH pore

diameter for SBA15 (9.9) if compared to SBA15 (6.7). IMC structure and particle morphology are shown by the XRPD pattern (Fig. 2-left b) and in the SEM image (Fig. 2-right b). Next we investigated the properties of IMC-loaded samples. In the first set of experiments we loaded the material with lower pore size with increasing amounts of saturated solution of IMC/acetone to probe the detectability of excess IMC deposited outside the pores by means of XRPD. Here we assume that XRPD cannot detect crystalline particles with sizes as small as the present pore size because the number of scattering centers in such a small particle is too low to assure detectable constructive X-ray interference. Thus, it is expected that samples with incompletely filled pores will exhibit amorphous XRPD patterns, whereas the excess of IMC deposited outside the pores will give detectable peaks. The XRPD patterns of IMC loaded SBA15 with the optimal loading where no peaks were observed and the lowest excess loading where they were observed are shown in Fig. 2-left, curves (c) and (d), respectively. These results are consistent with the corresponding SEM images (Fig. 2-right), where no IMC is observed in image (c) whereas IMC is observed in image (d).

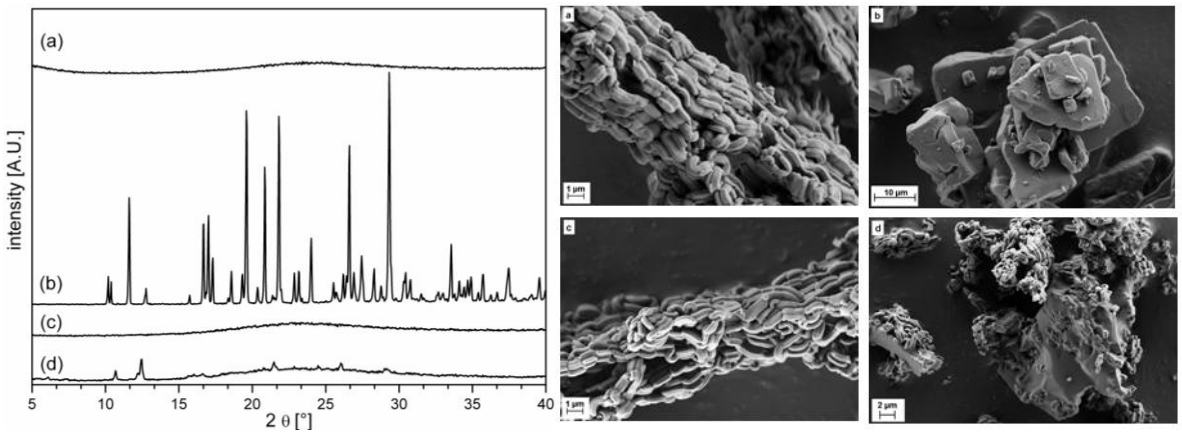

Figure 2: XRPD patterns of (a) pure calcined SBA15, (b) IMC, (c) with optimal IMC loading and (d) SBA15 loaded with excess IMC, with corresponding SEM images.

Excess amount of IMC deposited outside the pores was also detectable by means of SEM, although it took a lot of effort to find IMC (Fig. 2-right d). As seen from Fig. 2-left, XRPD is a suitable method for detection of excess amount of IMC deposited outside the pores. This enables the detection of total loading capacity in a single-step loading procedure using different solvents. Therefore we loaded both SBA15 silicates with increasing amounts of saturated solutions of IMC/acetone and IMC/ethanol and recorded XRPD patterns. The samples with optimal loading which had no peaks in their XRPD patterns were then investigated with DTA/TG focusing on the amount of residual solvents and total amount of loaded drug. The DTA/TG curves of these samples are given in Figure 3.

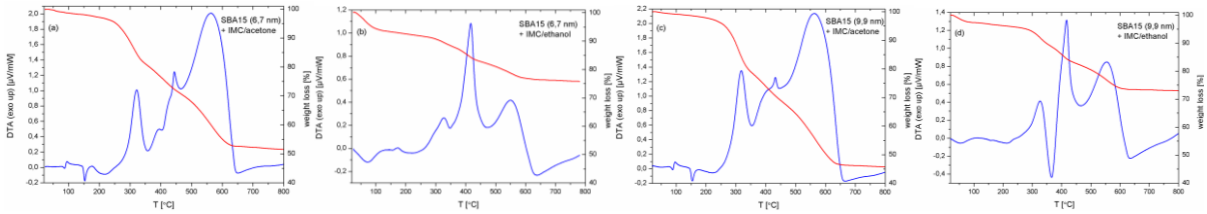

Figure 3: DTA/TG curves of SBA15 (6.7) loaded with IMC from (a) acetone and (b) ethanol, and curves of SBA15 (9.9) loaded with IMC from (c) acetone and (d) ethanol.

The thermal behavior can be divided into three regions. The first one represents an endothermic peak and the corresponding weight loss between 20 and 180 °C which is due to

the removal of residual solvent (in this case ethanol or acetone). In the DTA curves additional thermal events are observed which are due to thermal transitions of IMC and will not be pursued here, because structural and dynamical properties of the loaded drug are a matter of its own and will be carried out in detail in our future work. The second interval represents a second endothermic peak and a corresponding weight loss between 180 and 260 °C which is due to the removal of chemisorbed water (in form of isolated, geminal and vicinal silanol groups) accompanied by further condensation to Si-O-Si bridges. The third one, above 260 °C is due to combustion of organic constituents (in our case IMC). Regardless of the loading solvent used, three dominant exothermic peaks are observed, although with different ratios. It can be concluded that the combustion mechanism is not independent of the type of solvent used. The amount of residual solvent in SBA15 (6.7) was app. 1 % in the case of using acetone and app. 5 % in the case of using ethanol. In the case of SBA15 (9.9) the amounts were app. 1% and 6 %, respectively. A higher amount of residual ethanol may be explained by the ability of ethanol to act as a hydrogen bond donor and acceptor, while acetone can act as an acceptor only. This can cause stronger interaction of the former with surface silanol groups of SBA15. The amount of loaded drug was extracted from the weight loss in the third region. In the case of SBA15 (6.7) the amount of IMC was 43 %, where acetone was used, and 12 % where ethanol was used. In the case of SBA15 (9.9) the amounts of IMC were 49 % and 23 %, respectively. The general feature of much higher loading in the case where acetone was used is explained by means of much higher solubility of IMC in acetone. It is also found that the loading is higher in SBA15 with larger pore size and mesopore volume, regardless of the solvent used. The relatively small difference between loading into SBA15 with different pore sizes in the case of the same loading solvent is somewhat surprising with respect to the mesopore volumes. Namely the difference in mesopore volumes is much larger than the difference in the resulting loadings. This hints at the complex particle formation and embedding mechanism, which cannot be explained with plain SBA15 material properties as pore size and mesopore volume.

CONCLUSION

SBA15 silicates with average pore sizes 6.7 nm and 9.9 nm were prepared and loaded with various amounts of IMC by a single step loading procedure using acetone or ethanol as a loading solvent. It was shown that XRPD is suitable for detecting IMC deposited outside the pores. A general strategy was developed for determining the total amount of loaded drug using a combination of XRPD and DTA/TG. It was shown that the amount of residual solvent depends on the solvent properties and that the amount of loaded drug depends on the solvent used (i.e. the drug solubility) and the material characteristics (such as pore size and mesopore volume, specifically larger pore size and mesopore volume enables higher loading). It was also shown that there is no 1 to 1 correspondence between mesopore volume and total amount of loaded drug which indicates the complexity of the loading mechanism.

REFERENCES

[1] S. Wang, *Micropor. Mesopor. Mater.* 2009, **117**, 1-9.
[2] M. Vallet-Regi, L. Ruiz-Gonzalez, I. Izquierdo-Barba, J. M. Gonzalez-Calbet, *J. Mater. Chem.* 2006, **16**, 26-31.
[3] Andersson, J. Rosenholm, S. Areva, M. Linden, *Chem. Mater.* 2004, **16**, 4160-4167.
[4] Q. Yang, S. Wang, P. Fan, L. Wang, Y. Di, K. Lin, F.-S. Xiao, *Chem. Mater.* 2005, **17**, 5999-6003.
[5] J. L. Vivero-Escoto, I. I. Slowing, C.-W. Wu, V. S.-Y. Lin, *J. Am. Chem. Soc.* 2009, **131**, 3462–3463.